Mat. Res. Soc. Symp. Proc. Vol. 676 © 2001 Materials Research Society

The characterisation and reactivity of nanostructured cerium-copper-oxide composites for environmental catalysis

Othon Adamopoulos[1], Yu Zhang[1], Mark Croft[2], Igor Zakharchenko[3], Thomas Tsakalakos[3], Mamoun Muhammed[1]
[1]Dept of Materials Science and Engineering, The Royal Institute of Technology, Stockholm S-100 44, Sweden
[2]Dept of Physics, and [3] Dept of Ceramics and Materials Engineering, Rutgers University, Piscataway, NJ, U.S.A

ABSTRACT

Nanophase Ce-Cu-O powder has been synthesised via co-precipitation approach, whereas computer-assisted thermodynamic modelling was used to predict the optimum experimental criteria. The properties of Ce-Cu-O composite (10 mol% CuO) have been extensively investigated by a variety of techniques. The obtained materials show different morphology compared to other doped ceria salts, with uniform distribution of Ce and Cu throughout the powder. Detailed XRD study does not show the formation of solid solution and the composites consist of two separate metal oxides. X-ray absorption spectroscopy study shows a variation of the existence of Cu and Ce in several oxidation states. Copper oxide seems to exist evenly distributed along the surfaces and boundaries of the crystal grains of CeO_2 on the nanoscale. The temperature-programmed reduction indicated that Ce-Cu-O composite has an enhanced oxygen storage capacity compared to CeO_2 or pure copper oxide.

INTRODUCTION

The catalytic properties of some oxide ceramics and their solid solution derivatives are greatly dependent upon the particle size, the structural distortion and the chemical nonstoichiometry. When the grain size decreases below 100 nm, the density of the defects increases. Stoichiometric defects such as oxygen deficiency (vacancy) and its mobility on the catalyst surface are of great importance for redox gas reactions. Therefore, by doping ceria, CeO_2, with several isovalent or noniso-valent cations, its catalytic behaviour becomes more intense [1].

CeO_2 plays significant roles in several catalytic processes [2]. In recent years, it has been extensively used as a promoter in three-way catalysts (TWCs) for automotive emission control. Under various redox conditions, the oxidation state of cerium may vary between +3 and +4. Owing to its nonstoichiometric behaviour, CeO_2 has proved to be a good promoter for oxygen storage, while some noble metals are used as major catalysts. Related to the system of Ce-Cu, it has been reported that 10% of Cu gets doped in ceria lattice [3]. Herein it is reported, hardly is Cu fully doped in CeO_2 face centred crystal structure, and the physicochemical properties are investigated.

EXPERIMENTAL DETAILS

Computer modelling of chemical equilibrium was used to design the optimum co-precipitation conditions. The synthesis took place at specially constructed laboratorial synthesis reactor, where the addition of the solutions was accomplished simultaneously and automatically. Afterwards, the precipitate was washed and dried at 105 °C overnight. The precursor was calcined at 400°C, 500°C and 600°C for two hours.

The thermogravimetric analysis, the specific surface area and the density of the synthesised materials were studied with Perkin Elmer TGA 7, Gemini 2370 Surface Area Analyzer, and Pycnometer AccuPyc 1330, Micromeritics, respectively. The crystallographic study and the morphology of the particles were performed with Philips PW 1012/20 diffractor using Cu Kα1 radiation, and SEM Jeol JSM-880. The X-ray absorption spectroscopy (XAS) measurements were carried out in the fluorescence modes on beam lines X-19A and X-18B at the Brookhaven National Synchrotron Light Source, using Si (111) double crystal and channel cut monochromators. A standard was run simultaneously with all measurements for precise calibration. All spectra were normalized to unity step in the absorption coefficient from well below to well above the edge. The samples redox reactivity was examined by temperature-programmed reduction (TPR), using a Micromeritics TPD/TPR 2900 Chemisorption Analyser.

RESULTS AND DISCUSSION

A precursor containing Ce-Cu oxalate with molar ratio Ce:Cu=9:1 was obtained by the co-precipitation method. Thermogravimetric analysis showed that the precursor decomposes to oxide at temperatures above 330 °C. A sample of the precursor was therefore calcined at different temperatures; 400°C, 500°C and 600°C for two hours. The density, the specific surface area, the particle size distribution, the morphology and the crystallographic phases of the precursor and the calcined material were investigated (c/f Table I).

According to Table I, the calcination of the precursor results in the decrease of the particle size. The crystallite size, as determined from the XRD data, increases with the calcination temperature. The much larger particle size -as determined by DLS method and specific surface area (BET) method- compared to the crystallite size indicates the existence of agglomeration. The agglomerates observed at SEM, FEM and TEM show the particles to be shaped into fine sheet-rod-like with aspect ratio 4-10. The elemental distribution on these particles was homogeneous, as shown from the electron backscattering in SEM micrographs (Fig. 1c). The lattice parameter (a) of the calcined materials (both CeO_2 and Ce-Cu-O) is the same, indicating that Cu is probably not dissolved in the ceria phase.

Table I. Comparison of some physical properties of Ce-Cu-O (9:1) and ceria.

Physical properties	**Ce-Cu-O**				**Ceria(1)**	
	Precursor	**Calcined at**			**Precursor**	**Calcined at**
		400 °C	500 °C	600 °C		600 °C
Density(2) (g/cm^3)	2.80	6.37	6.32	7.22	2.70	7.00
Specific surface area (m^2/g)	3	39	51	33	3	38
Particle size (nm)						
• From XRD	-	7	9	12	-	15
• From BET	679	24	19	25	652	23
• DLS(3)	-	620	728	657	-	786
• SEM width (μm)	0.8	0.3	0.5	0.4	1.2	0.4
length (μm)	2.3	1.4	1.8	1.7	3.1	2.5
Lattice parameter a (nm)	-	0.5409	0.5401	0.5405	-	0.5405

(1) Sample prepared in identical manner to Ce-Cu-O sample; (2) theoretical density of ceria 7.216 g/cm^3 from literature; (3) dynamic light scattering technique.

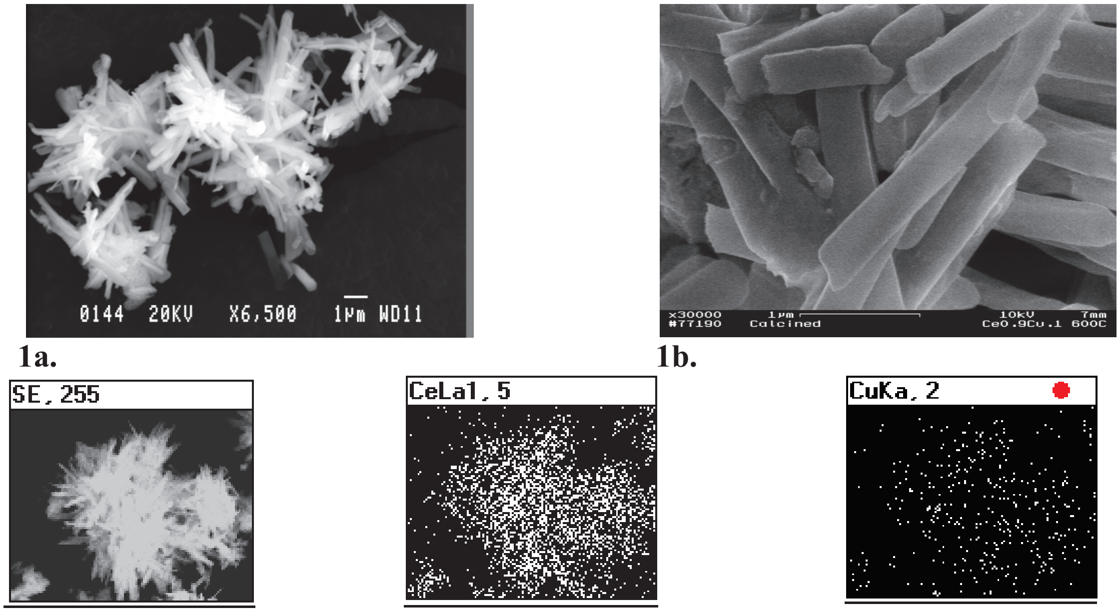

1a. 1b. 1c.

Figure 1. SEM and FEM micrographs of calcined powder at 400^{o}C and 600^{o}C. The particles were shaped into fine sheet-needles with aspect ratio 4-10. The SEM electron backscattering for the calcined sample at 400^{o}C for two hours shows a homogeneous elemental distribution.

XRD study

The precipitated Ce:Cu oxalate (9:1) is x-ray amorphous, while the oxalate precipitation of either Ce or Cu alone is a crystalline powder (Fig 2.). This indicates that the precipitated Ce-Cu oxalate is metastable and the mixing of the Ce, Cu and oxalate on the atomic scale is probably the reason for the disordering of the powder.

By careful analysis of the XRD data, it is seen that two weak peaks, characteristic for CuO, appear at 35.63^{o} and 38.85^{o}. Due to the low concentration of Cu in the sample, it is difficult to clearly identify these two peaks. Therefore, we have collected x-ray diffraction data using a strong radiation source (at the Brookhaven National Laboratory). The inset of Fig. 2 shows the existence of these two peeks. By semi-quantitative analysis of the data, we estimated that the entire Cu-containing mixed oxides exists as CuO and not as a solid solution.

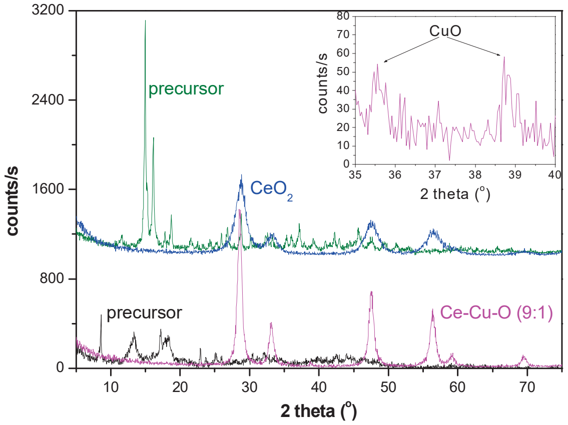

Figure 2. XRD patterns of pure ceria and Ce-Cu-O (9:1) calcined at 600^{o}C. The CuO peaks can be observed at 35.63^{o} and 38.85^{o}.

XAS study

In order to investigate the Ce-Cu-O system a detailed study using XAS has been undertaken. The technique is especially suited for the determination of the oxidation state (valance) of rare earth compounds. Two samples were used in this study; the precursor and the sample calcined at 600°C.

Ce-L$_3$ XAS. The Ce-L$_3$ edges of the precursor and the calcined samples are plotted in Fig. 3. The R-L$_3$ edges are dominated by a sharp "white line" (WL) feature, due to 2p to 5d atomic like transitions. Unstable valence rare earth elements can support f-configurations, which differ by one 4f electron. The XAS spectrum of mixed valence rare earths manifest separate f^{n+1} and f^n WL features split by 7-10 eV. This splitting is due to the additional Coulomb interaction energy between the 2p-core hole (in the XAS final state) and the excess 4f-electron in one of the configurations. The relative strengths of the f^n and f^{n+1} related WL XAS features scale with the weights of these states in the initial configurations. The Ce-Cu oxalate spectrum manifests a single robust WL feature at the edge, typical of a pure Ce^{3+}- $4f^1$ state. By contrast, the Ce-Cu-O WL (Fig. 3 and inset) exhibits a couple of distinct peaks (A and B) associated with the Ce^{4+}- 4 f^o and Ce^{3+}-4 f^1 configurations.

The extended spatial character of the Ce-4f orbital leads to strong hybridisation/co-valency effects and to substantial f^1 weight in Ce^{4+} compounds. Specifically, note in Fig. 3 the large f^1 related feature (B_1-B_2 in the inset), despite the formally Ce^{4+} state of CeO_2. Within cluster model calculations, this co-valency is manifested by the admixture of the $4f^1L$ configuration (where the L refers to a ligand - O hole) into the Ce electronic configuration [4]. After this convention, the B_1-B_2 feature of the Ce-Cu-O is labelled with the $4f^1L$ label in Fig. 3. The strongly bimodal (A-B) WL feature of the Ce-Cu-O spectrum is clearly an indicator of formally the Ce^{4+} state. Since insulating Ce^{3+} compounds also exhibit their first WL-peak at the energy of the precursor peak (Fig. 3) the pronounced chemical shift to higher energy of the Ce-Cu-O sample spectrum is also a signature of the formally Ce^{4+} state.

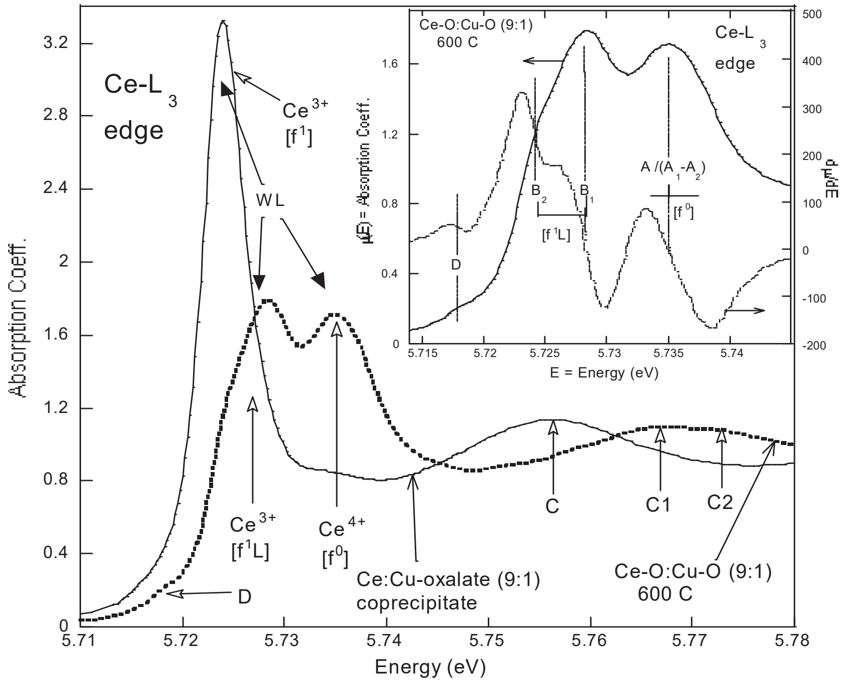

Figure 3. The Ce-L$_3$ edges of Ce-Cu precursor sample and Ce-Cu-O calcined at 600°C. The weak D feature should be noted. Inset: The derivative of the absorption coefficient (μ) with respect to energy dμ/dE for the Ce-L$_3$ edge spectra of the Ce-Cu-O calcined at 600°C for two hours.

Cu-K XAS. Fig. 4 shows the Cu-K edges of the Ce-Cu oxalate, the Ce-Cu-O calcined at 500°C and 600°C, and few standard compounds. Although weekly broadened, the spectra of the Ce-Cu-O oxides clearly coincide spectral-feature-for-spectral-feature and in chemical shift precisely with the CuO spectrum. Therefore, it is deduced that the Cu in these materials occurs as CuO with other components being below the detection level. The spectrum of Ce-Cu oxalate is clearly strongly shifted to lower energy compared to that of CuO.

Origin of Ce^{4+} and Cu^{+} in the mixed sample.

The precursor contains only Ce^{3+} and Cu^{2+} ions. The formation of Ce^{4+} and Cu^{+}, indicated by the EXAFS study, must therefore have been formed as a result of the decomposition reactions taking place during calcination, as given below:

$$Ce_2(C_2O_4)_{3(s)} \rightarrow Ce_2O_{3(s)} + 3CO_{(g)} + 3CO_{2(g)} \rightarrow 2CeO_{2(s)} + 4CO_{(g)} + 2CO_{2(g)} \qquad (1)$$

$$CuC_2O_{4(s)} \rightarrow CuO_{(s)} + CO_{(g)} + CO_{2(g)} \qquad (2)$$

Nevertheless, under atmospheric air the following reaction is kinetically faster than the last step of reaction (1):

$$Ce_2O_{3(s)} + \tfrac{1}{2}O_{2(g)} \rightarrow 2CeO_{2(s)} \qquad (3)$$

On the other hand, the existence of $CO_{(g)}$ may reduce Cu^{2+} to Cu^{+} as follows:

$$2CuO_{(s)} + CO_{(g)} \rightarrow Cu_2O_{(s)} + CO_{2(g)} \qquad (4)$$

while Cu^{+} is oxidised to Cu^{2+} in air:

$$Cu_2O_{(s)} + \tfrac{1}{2}O_{2(g)} \rightarrow 2CuO_{(s)} \qquad (5)$$

Thereby, we have two metal oxide systems, each one existing in two different valences, i.e. Ce^{3+}/Ce^{4+} and Cu^{+}/Cu^{2+} depending upon the atmosphere.

Temperature-programmed reduction of Ce-Cu-O system

The results of the TPR study for three different samples, i.e. CeO_2, CuO and CeO_2-CuO (mole ratio=9:1), are shown in Fig. 5. The temperatures at which the reaction with H_2 starts up (T_{up}) for CeO_2 and CuO are 200°C and 300°C, respectively. However, the T_{up} for CeO_2-CuO is also 200°C, likely because of the reduction of CuO by H_2 at first, as follows:

$$2CuO_{(s)} + H_{2(g)} \rightarrow Cu_2O_{(s)} + H_2O_{(g)} \qquad (6)$$

Then, Cu_2O, which is possibly distributed on the surfaces or boundaries of CeO_2 grains, may reduce CeO_2, according to reaction (7):

$$CeO_{2(s)} + \delta Cu_2O_{(s)} \rightarrow CeO_{2-\delta(s)} + 2\delta CuO_{(s)} \qquad (7)$$

Reaction (7) appears more effective than in the case H_2 reduces directly pure CeO_2:

$$CeO_{2(s)} + \delta H_{2(g)} \rightarrow CeO_{2-\delta(s)} + \delta H_2O_{(g)} \qquad (8)$$

Therefore, the TPR peak of CeO_2-CuO is shifted to lower temperature than that of CeO_2. That is to say, CuO plays a role of a catalyst at -relatively- low temperature for the reduction of CeO_2. Thus, due to the enhancement of the redox activity of Ce-Cu-O, this mixture could be used as a catalyst for gas redox conversion at lower temperature.

CONCLUSIONS

- The co-precipitation of cerium and copper by oxalate ligand produces a metastable composite of Ce-Cu-oxalate (mole ratio 9:1), which is X-rays amorphous. The precursor was calcined to produce nanocrystalline metal oxide powders.
- Careful XRD study of Ce-Cu-O reveals that Cu-O forms no solid solution with CeO_2.
- XAS study showed the existence of Ce^{3+} and Ce^{4+}, as well as Cu^{+} and Cu^{2+} in the calcined powder.

- TPR studies showed an enhanced catalytic reactivity of the Ce-Cu-O system. This is explained by the interaction of the double redox system $Ce^{3+/4+}$ and $Cu^{+}/^{2+}$.

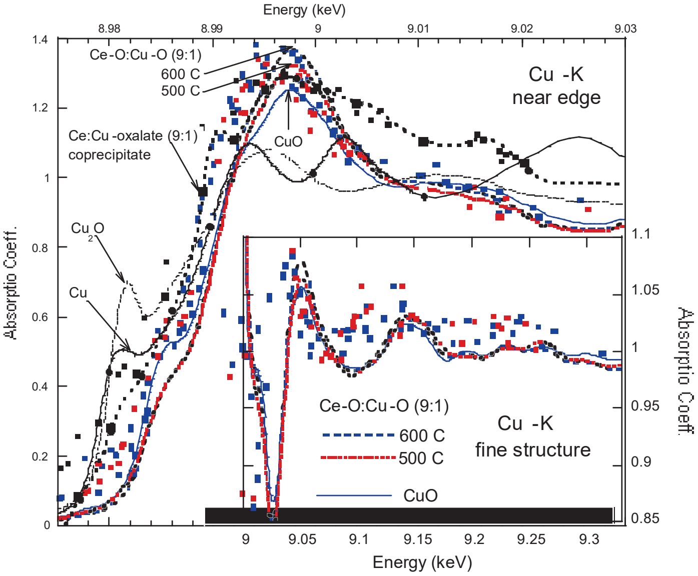

Figure 4. The Cu-K edges of the Ce-Cu oxalate (9:1) co-precipitated powder, the Ce-Cu-O calcined at 600°C and 500°C, and few standard compounds. Inset: the fine structure above the Cu-K edge for the calcined powder at 500°C and 600°C, and for CuO.

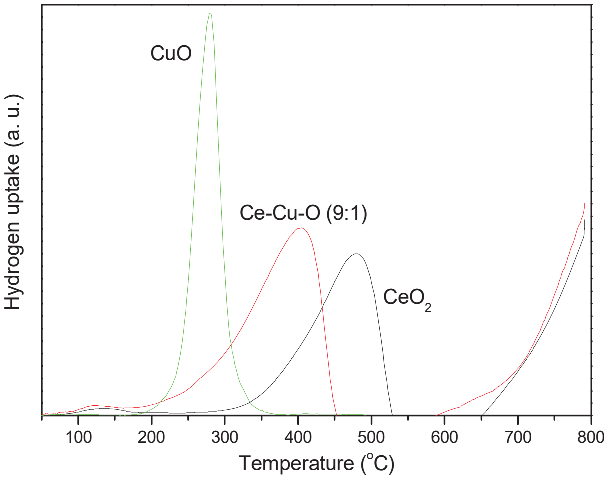

Figure 5. The results of the TPR study for three different samples, i.e. CeO_2, CuO and CeO_2-CuO. The temperatures at which the reaction with H_2 starts (T_{up}) for CeO_2 and CuO are 200°C and 300°C, respectively. Notwithstanding, the T_{up} for CeO_2-CuO is also 200°C, probably due to the reduction of CuO by H_2.

ACKNOWLEDGEMENTS

The work has been - in part - financially supported by dmc² (formerly Degussa), Germany.

REFERENCES

---

1. C. Palmqvist, E. M. Johansson, S. G. Järås and M. Muhammed, *Cat. Lett.* **56**, 69-75 (1998).
2. K. Bak and L. Hilaire, *Applied Surface Science* **70/71,** 191 (1993).
3. Y. Zhang, S. Andersson and M. Muhammed, *Applied Catalysis B* **6**, 325-337 (1995).
4 A. Solatov, T. Ivanchenko, S. Longa, A. Kotani, Y. Iwamoto and A. Bianconi, *Phys. Rev.* **B50**, 5047 (1994) and references therein.